Assessment of the properties of Diethyl phosphite as a novel anticorrosion pigment in organic coatings

[a]Kateřina Nechvílová, [a]Andréa Kalendová, [b]Eva Schmidová, [c]Patrycja Bober

[a] *Faculty of Chemical Technology, Department of Chemistry and Materials Technology, Univerzity of Pardubice, Studentská 95, 53210 Pardubice, Czech Republic*

[b] *Jan Perner Transport Faculty, Educational and Research Centre in Transport, Univerzity of Pardubice*

[c]*Institute of Macromolecular Chemistry AS CR, Department of Conducting Polymers, Heyrovsky Sg. 2, 16206 Prague, Czech Republic*

Corresponding author: Ing. Kateřina Nechvílová; *E-mail adress:* Katerina.Nechvilova@seznam.cz

Received []

The aim of this work was to provide a first description of the behaviour of diethyl phosphite in organic coatings. Description of their physico-mechanical properties as well as anticorrosion properties in the protection of steel substrates. The diethyl phosphite behaviour in the organic coatings depends on the volume concentration of the pigment. A polyaniline base was suspended in diethyl phosphite as a new reactant. The pigment so prepared was used as a corrosion inhibitor in model paints containing a solvent-based epoxy-ester resin as the binder. The organic coatings were applied to steel panels and to glass panels and subjected to mechanical tests, corrosion resistance tests and electrochemical tests. Furthermore, they were exposed to the environments of condensed steam, neutral salt solution mist, and sulphur dioxide-containing mist. The corrosion effects were evaluated and the organic coatings' overall anticorrosion efficiency was calculated from the results. Ultimately, the optimum pigment volume concentration (PVC) at which the coatings provided the best anticorrosion protection was determined: it was PVC = 10 vol. %, whereas the best mechanical resistance was observed at PVC = 5 vol. %. The goal of the forthcoming work will be to optimise all the properties into a single pigment volume concentration.

Keywords: Diethyl phosphite, conductive polymers, polyaniline, organic coatings

Introduction

Conductive polymers are well known devepoling materials. These substances are still extensively investigated. (Shauer et al., 1998) not only for their good properties such as good stability in the environment and optical properties (Huo et al., 1999) but, in particular, for their own electric conductivity, which is closely related to the conjugated double bond system in the macromolecular chains (Olad et al., 2013). Scientific literature reflects the wide interest in such materials, which can be prepared by several feasible procedures and methods. The most widely used methods use the polymerisation approach (Cruz-Silva et al., 2004) and the electrochemical approach (Montheo et al., 1998). Prominent compounds in the conductive polymer class include polyacetyl, polypyrrole, polythiophenylenes, poly(*p*-phenylenes) and, in particular, polyanilines and their derivatives (Shauer, 1998; Ates et al., 2004).

Stainless steel on the carbon steel base products have been widely used directly in various fields. These materials have excellent mechanical performance, corrosion resistance and other characteristics (Liu et al., 2013). Therefore this paper is focused on the steel protection with using conductive polymer.

Polyaniline (PANI) has been in the focus of researchers (Ozyilmaz et al., 2014; Tokarsky et al., 2014) especially owing to its outstanding electric conductivity, high stability, easy synthesis, low costs of the incoming raw materials (Ayad et al., 2003), and redox properties, described by Jing Luo et al. in 2007 (Luo et al., 2007). The first papers dealing with PANI were published in 1985, and a lot of work has concentrated on its properties and potential uses since then (Yang et al., 2010). PANI has a very broad applicability scope: it is used in gas sensors and biological sensors, rechargeable batteries, solar cells and diodes, electrochromic screens, anticorrosion paints, and in many other areas of technology (Bedekar et al., 1997; Elkais et al., 2011). Specifically in the anticorrosion protection field, PANI has been studied for over 30 years and has been superseding toxic pigments, so popular in the past (Ozyilmaz et al., 2014). The corrosion potential and stainless steel protection against corrosion by means of PANI coatings were described by Deberry in 1985. Thereafter, other metals protected with such coatings were described as well: iron (Yang et al., 2010), aluminium (Navarchian et al., 2014), copper, zinc (Ozyilmaz et al., 2014), various alloyed structures (Ozyilmaza et al., 2013). Organic coating materials started to be developed. One of the first studies of electrochemically prepared PANI films with smooth surfaces was performed by Diaz (Montheo et al., 1998), Abu and Aoki described paints based on various latex types (Yang et

al., 2010), Olad and Rashidzadeh (Olad & Rashidzadeh, 2008), and also Špírková (Špírková et al., 2008), made use of the anticorrosion properties of PANI/OMMT (organically modified montmorillonite) based films. Based on that work, Navarchian developed nanocomposites with kaolin particles (Navarchian et al., 2014). Other ingredients followed, e.g. graphite (Kulhánková et al., 2014), fullerenes (Sapurina et al., 2000), silicates (Kalendová et al., 2014), and many other combinations.

Polyaniline, having a general formula $[(-B-NH-B-NH-)_y(-B-N-Q-N-)_{1-x}]_x$, comprises a benzoid structure (B) and a quinoid structure (Q) (Olad et al., 2013), specifically phenylene and quinone diimine structures (Luo et al., 2007). It can exist in 3 oxidation states depending on the protonation/deprotonation status of the molecule (Mousavinejd et al., 2015). The colour transitions between those species were described by Chiang & MacDiarmid, 1986. The 3 species are emeraldine (green; half-oxidised, $y = 0.5$), leucoemeraldine (yellow; fully reduced, $y = 0$), and pernigraniline (violet; fully oxidised, $y = 1$) (Elkais et al., 2011). Doping and, at the same time, conductivity of the PANI chain are provided by inorganic Brönsted acids (Dispenza et al., 2015) (HCl, H_2SO_4, H_3PO_4, HBF_4) and organic acids (camphoric acid, 5-sulphosalicylic acid (Liu et al., 1999) or dodecylbenzenesulphonic acid), where the organic acid enhances solubility (Ayad et al., 2008). Of the 3 species, the green emeraldine salt (ES) is the most important one. PANI is conductive in this form but it is soluble, and therefore it is converted to the insoluble emeraldine base (EB) (Liu et al., 1999). The base can be fully used for anticorrosion purposes, as confirmed by Spinks, et al. 2003.

PANI is synthesized by chemical oxidation of aniline or an aniline salt in acid aqueous environment, using ammonium peroxodisulphate, $FeCl_3$, dichromates, permanganates or hydrogen peroxide as the oxidant. The oxidants are capable of forming radical cations, which can react with the aniline molecules in the pernigraniline form, bringing about polymeric chain extension (Ayad et al., 2003). Protonation with an acid gives rise to p-charged carriers. Protonation occurs on the imine groups first, resulting in the formation of relatively stable radical cations with delocalised p-positions and conjugated π-bonds, which are responsible for the material's electric conductivity. The charges of the radical are compensated by the appropriate anion (Shauer et al., 1998; Ayad et al., 2008). From among organic solvents, xylene, chloroform, *m*-cresol, dimethyl sulphoxide or *N*-methyl-2-pyrrolidinone can be used (Cruz-Silva et al., 2004). They are media in which the PANI powder of the emeraldine base can be dissolved.

Corrosion is an adverse process that can be prevented by using organic coatings (Olad et al., 2013). The anticorrosion protection mechanism when using PANI is anodic by nature. The substrate metal's potential is shifted in the positive direction to the passivating region where the corrosion current is very low. Active protection is provided due to the reverse redox-catalytic PANI properties, and so PANI can facilitate the formation and stabilisation of the protective oxide layer at the metal/paint interface, consisting of Fe_3O_4 on the metal side and γ-Fe_2O_3 on the coating side (Shauer et al., 1998). The reduced PANI can be oxidised back by oxygen which is present in the system. PANI increases cathodic resistance, the metal surface pH being the limiting factor. The emeraldine salt acts as a buffer by absorbing the hydroxyl ions produced during cathodic oxygen reduction. PANI must be in galvanic contact with the substrate metal for the protection to be efficient. The next protective mechanism consists in the barrier effect, where the PANI pigment particles or particles of other fillers at low concentrations prevent the corrosive medium from penetrating to the substrate metal (Olad et al., 2013; Jafarzadeh et al., 2016).

Diethyl phosphite $(C_2H_5O)_2P(O)H$ is a phosphorous acid salt. It is a colourless substance, soluble in water, amply used, e.g., as a reductant (Gong et al., 2009; Laymonie, 2007). It has never been used in the area of paints and its use with PANI has not been described. The aim of this work was to get first information on the properties of a newly prepared pigment comprising diethyl phosphite with the polyaniline base (referred to as DEPh/PANI), and to prepare paint films containing DEPh/PANI and examine their anticorrosion efficiency. Based on the facts ascertained, a DEPh/PANI paint film was obtained exhibiting the highest anticorrosion efficiency and the highest adhesion to the substrate.

Experimental

Description of the pigment

Polyaniline was prepared by standard oxidation of 0.2 M aniline hydrochloride with 0.25 M ammonium peroxodisulphate in an aqueous medium at room temperature (Stejskal et al., 2002). The solids were then converted to the PANI base in a 1 M ammonium hydroxide solution. Drying in air and then on silica gel at room temperature followed. The PANI base was suspended in diethyl phosphite without using any organic solvent or water. The reaction was accompanied by colour changes, from dark blue to the final dark (emerald) green. The final substance was filtered out, rinsed with ethanol and dried in air and on silica gel.

The basic pigment properties were determined pycnometrically (AccuPyc II 1340 Pycnometer, USA) with a precision to 3 decimal places (CSN ISO 787−10). The critical pigment volume concentration (CPVC) was determined via linseed oil absorption (Oil abs) per 100 g of the pigment (CSN ISO 787−5) by the pestle-and-mortar method as per CSN 67 0531. The CPVC value served to set up a concentration series. DEPh/PANI pigment particle morphology and shape, Fig. 1 were examined on a JEOL-JSM 5600 LV (Japan) electron microscope.

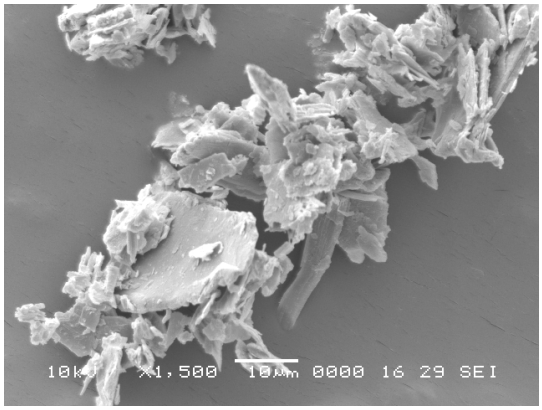

Fig. 1. Electron microscopic photograph of the DEPh/PANI pigment particles, magnification 4.5 thousand-fold.

The conductivity (χ) and pH levels of a 10 % pigment suspension in redistilled water were measured during 21 days as per CSN ISO 789−9 and CSN ISO 787−14. The suspension was then filtered and a steel panel was immersed in it and exposed to its action for another 21 days. The steel weight loss values were measured in dependence on the medium containing protective substances released from the pigments. Matter soluble in hot water and in cold water was also determined (CSN ISO 787−3 and 787−8, respectively).

Paint formulation and preparation

A solvent-based epoxy-ester resin was used as the binder. The paints were prepared by dispersing the pigment in the binder at pigment volume concentrations (PVC) 1 vol. %, 3 vol. %, 5 vol. %, 10 vol. %, 15 vol. % and 17 vol. %. (Note. in the following text, the symbol DEPh/PANI_n denotes a paint with the DEPh/PANI pigment present a PVC = *n*.vol. %.) The paints were homogenised in a Dissolver at 3000 rpm for 45 minutes. The non-pigmented epoxy-ester resin (nER) and a paint containing polyaniline hydrochloride (PANI/HCl) at PVC = 5 vol. % served as reference materials.

The binder was the commercial product WorléeDur D 46 (Worlée-Chemie, Germany), which is a short epoxy-ester resin containing drying fatty acids.

Analytical data:	Epoxy resin fraction:	~60 %
	Oil components:	~40 %
	Acid value:	≤4
	Density:	0.98 g cm^{-3} (20 °C)

The paints were applied to clean and degreased glass and steel panels (Q-LAB Corporation, UK) by means of a box-type ruler. The 250 µm slit was used for the first coat, the next coats (for the anticorrosion tests) were applied depending on the film thickness (measured with a BYK Gardner, Germany, magnetic thickness gauge) as per CSN EN ISO 2808 so that the final paint film thickness was ≤ (200 ± 20) µm.

Paint film parameter testing

The paint film testing methods are destructive methods. The tests, described below, were selected so as to evaluate the paint films' physico-mechanical and anticorrosion properties.

Physico-mechanical tests

Physico-mechanical tests are destructive tests aimed at estimating the parameters contributing to the paint film's resistance, i.e. strength, elasticity and flexibility. Those parameters are used when inferring the organic coating's protective mechanism. The physico-mechanical tests were performed on steel panels 76 mm × 75 mm × 0.8 mm size (standard S-36 low-carbon steel, Q-LAB Corporation, UK). The mechanical properties of the paint systems were determined in line with applicable standards.

The paint film's adhesion was determined by the cross-cut method as per CSN EN ISO 2409. A cutting knife with blades 2 mm apart was used to create a square-shaped lattice having a defined area. The paint film was cut through down to the substrate. The cut overlaps, the lattice pattern, were assessed on a 0 to 5 scale where 0 denotes the highest paint film resistance.

The paint film's resistance to a falling weight was determined as per CSN EN ISO 6272. A 1000 g was allowed to fall freely on the front and back sides of a coated steel panel. The outcome was the largest fall height at which the film still remained undamaged.

The test on an Erichsen apparatus as per CSN ISO 1520 was aimed at determining the resistance of the paint film coated on a steel surface to indentation with a steel ball 20 mm in diameter.

The bending test was performed in accordance with CSN ISO 1519. The coated panel was bent over a steel mandrel, and the smallest mandrel diameter at which the paint film still remained undisturbed was recorded.

The overall physico-mechanical resistance of the paint films was calculated as the arithmetic mean of the scores attained in the tests.

Relative surface hardness of the paint film was determined as per CSN 67 3076 based on the time of pendulum dampening from 0.209 rad to 0.007 rad by using an Electrometer® Perzos instrument (UK) and from 0.105 rad to 0.005 rad by using a König instrument (BYK, Germany). This surface hardness relative to a glass standard (%) was measured during 200 days.

The pull-off test was performed on a steel panel for mechanical tests to which a steel target (20 mm in diameter) was fixed with a two-component adhesive (methyl methacrylate/dibenzoyl peroxide 10 : 1) and loaded with a 1000 g mass which was allowed to act for $\geq$ 2 h. The pull-off test was performed on a COMTEST®OP3P instrument (Czech Republic) at 800 kPa s^{-1} applying a limiting force of 15 kN.

The paint film properties on a nanometer scale were examined on an atomic force microscope (SOLVER-NEXT, Russia). A topographic image (Fig. 2) was obtained by using the atomic force microscope in the semicontact mode (NSG10 tip, k = 3.1−37.6 N m^{-1}). The scanned area was 20 × 20 μm, scanning rate 0.1 Hz, image resolution 512 × 512 points. Both the DEPh/PANI samples and the HCl/PANI reference samples were subjected to topographic scanning, nanoscratch tests and Young's modulus measurements. The modulus of elasticity of the nonpigmented epoxy-ester film was measured on a Hysitron TI 950 TriboIndenter™ by applying the CMX (Continuous Measurement of X) dynamic mode.

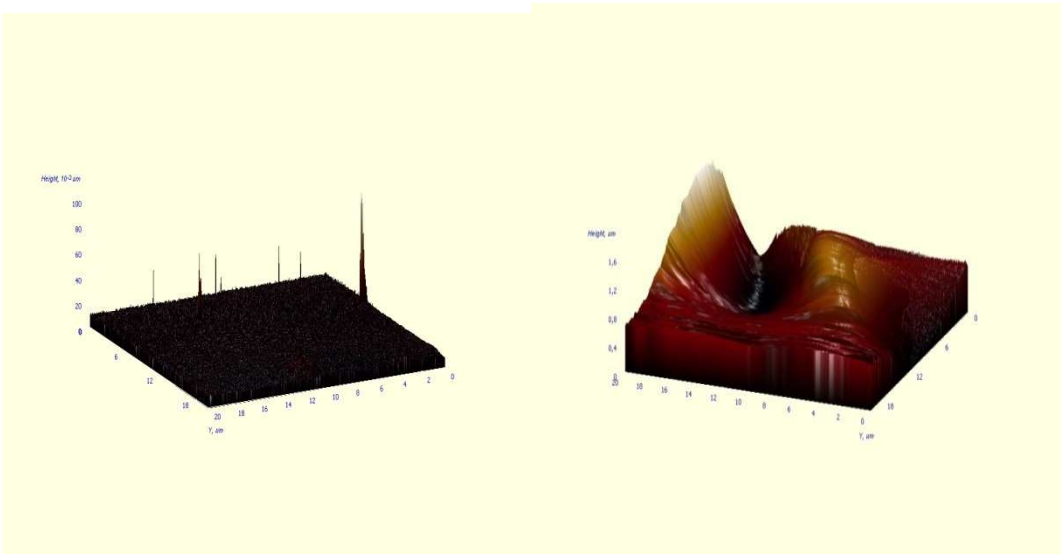

a **b**

Fig. 2. AFM topography image (scanned area 20 × 20 µm). Sample: (a) DEPh/PANI_1; (b) HCl/PANI

Corrosion tests

Accelerated corrosion tests are among the most important tools to gain insight into the anticorrosion properties of organic coatings. Such tests in laboratory conditions simulate various corrosion conditions in which the paint films are deliberately degraded.

Three different corrosion atmospheres types were used: condensed steam atmosphere, atmosphere of condensed steam combined with neutral salt spray, and atmosphere of condensed steam combined with SO_2. The tests were performed on steel panels 152 mm × 102 mm × 0.8 mm size (normal S-46 low-carbon steel, Q-LAB Corporation, UK). The first coat was applied with a box-type ruler with a 250 µm slit, the second coat was applied depending on the dry film thickness (DFT) of the first coat, measured with a magnetic thickness gauge. A test cut approximately 7 cm long and passing vertically through the film as deep as the substrate metal was made in each film for examination of the corrosion phenomena.

The following corrosion phenomena were examined after exposure to the corrosive environment (CSN EISO 4628−2 to 4628−5): blisters on the film surface (ASTM D 714−78), corrosion in the test cut (ASTM D 1654−92), and corrosion of the steel surface after removing the paint film (ASTM D 610−85). ASTM D 714-87 Method classifies the osmotic blisters formed to groups defined by the sizes designated by 2, 4, 6 and 8 values (2 denoting the highest size, 8 the lowest size). To the blister size an information is attached giving the

respective frequency of appearance. The highest frequency of appearance is designated as D (denoting dense), a lower one as MD (denoting medium denstity) and as F (denoting few). This approach can give a series starting with a surface showing the lowest corrosion attack by few osmotic blisters of small size up to dense large-size blisters. The anticorrosion efficiency (AE) was calculated for each corrosive environment as the arithmetic mean of the scores estimated for each corrosion effect, and the overall anticorrosion efficiency (OAE) was calculated as the arithmetic mean of the three anticorrosion efficiency values. And finally, the overall anticorrosion efficiency from the accelerated corrosion tests was combined with the score from the physico-mechanical tests to obtain the combined anticorrosion efficiency (CAE).

Accelerated cyclic corrosion test in the atmosphere combining salt spray with condensed steam (CSN EN ISO 9227)

The samples were exposed to the atmosphere in the test chamber in 12-h cycles comprising 6 h of exposure to a 5 % salt solution spray (pH 6.5−7.2) at 35 °C ± 2 °C, 2 h of exposure at 23 °C ± 2 °C, and 4 h of exposure to condensed moisture at 42 °C ± 2 °C. The total exposure time was 1344 h (Fig. 3).

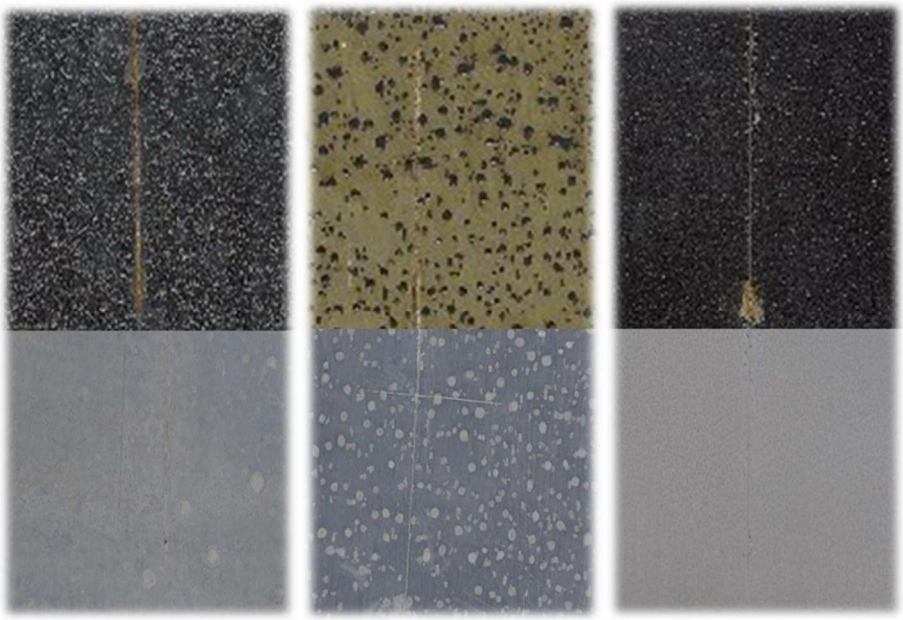

a **b** **c**

Fig. 3. Paints films containing (a) DEPh/PANI_10; (b) WorléeDur; and (c) HCl/PANI after 1344 h of exposure in the chamber with NaCl spray. One-half of each film was stripped to show corrosion of the substrate metal surface.

Accelerated cyclic corrosion test in the atmosphere with SO_2 mist and condensed steam (CSN ISO 6988)

The samples were exposed to the atmosphere in the test chamber in 24-h cycles comprising 8 h of exposure to SO_2 at 35 °C ± 2 °C followed by 16 h of exposure to condensed humidity at 21 °C ± 2 °C. The sample condition was evaluated in 1368 h of exposure (Fig. 4).

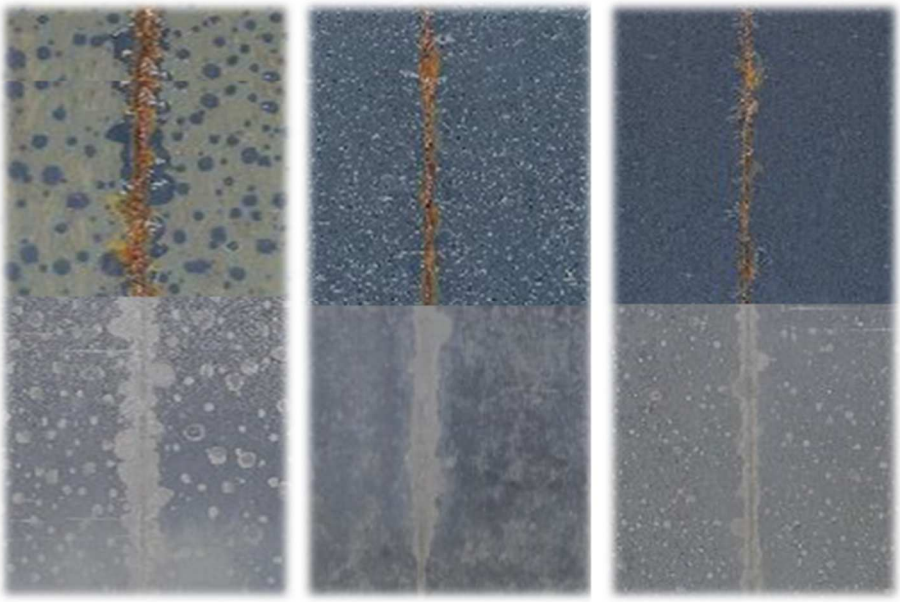

a **b** **c**

Fig 4. Paints films containing (a) DEPh/PANI_10; (b) WorléeDur; and (c) HCl/PANI after 1366 h of exposure in the chamber with SO_2 mist. One-half of each film was stripped to show corrosion of the substrate metal surface

Corrosion test in the condensation chamber with continuous moisture (CSN EN ISO 6270−1)

The organic coatings are exposed continuously to condensed steam at 38 °C ± 2 °C for 3552 h (Fig. 5).

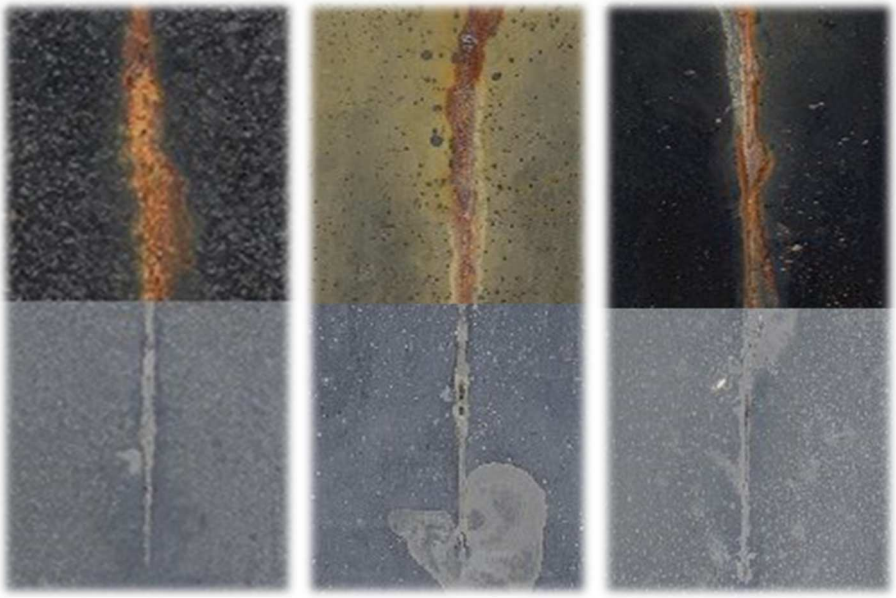

a **b** **c**

Fig. 5. Paints films containing (a) DEPh/PANI_10; (b) WorléeDur; and (c) HCl/PANI after 3552 h of exposure in the chamber with condensed moisture. One-half of each film was stripped to show corrosion of the substrate metal surface.

Accelerated weather test with UV radiation and controlled water condensation (CSN EN ISO 4892)

The organic coatings were placed in a QUV test chamber and subjected to repeated cycles comprising 4 hours of exposure to UV radiation at 60 °C ± 2 °C and 4 h of exposure to steam condensation in darkness at 50 °C ± 2 °C. The samples were exposed during a total of 500 h and then evaluated as per ASTM D 6625−13.

.

Linear polarisation

Linear polarisation was measured electrochemically by using a system comprising a reference electrode (ISE), a Pt cathode and a working electrode (anode). A 3.5 % NaCl solution was used. The corrosion rate C_R [mm year^{-1}] was calculated by using Eq. (1).

$$C_R = \frac{I_{corr}\, K\, EW}{\rho\, A} \quad (1)$$

The Eq.1 calculated with these components: I_{corr} - corrosion current [A]; K - constant that defines the unit of the corrosion rate; EW - equivalent weight, for the corrosion of iron Fe → $Fe^{2+} + 2^{e-}$ EW = 55.85/2 = 27.925 g/equivalent; ρ - density [g cm^{-1}]; A - sample area [cm^2].

Elemental microanalysis

Electron microanalysis for ascertaining the elemental composition of the paint films was performed on a TESCAN VEGA 5130SB scanning electron microscope and a Bruker Quantax 200 energy dispersive X-ray spectrometer. Electron microanalysis allows information on the concentrations of the elements to be obtained based on comparison of their spectral lines in the X-ray region with those of the standards.

Results and discussion

First, it is noteworthy that the film of the nonpigmented epoxy-ester resin (nER) provides a 100 % resistance from the physico-mechanical aspect. But although the overall physico-mechanical resistance is reduced by adding the DEPh/PANI pigment, it is especially the anticorrosion resistance that is higher with the newly created paint films.

The overall physico-mechanical resistance decreases as much as 8 % with increasing DEPh/PANI PVC (Table 1). The poorest results were obtained in the test of free weight fall on the back side of the painted panel – the result was 10 cm lower for PVC = 3 vol. % than for PVC = 0 vol. % (= nER). The limiting value was 50 cm height resistance to the free fall of a 1000 g mass observed with the HCl/PANI reference coating. Pain film elongation increased by as much as 14 % with increasing pigment concentration. The paint film was tough and a larger force was needed to pull the film or a part of it off the steel panel. Generally, the paint films were highly resistant (highly adhesive to the substrate). A 100 % cohesion fracture was only observed for DEPh/PANI_10, while only a part of the paint film tore off at the coating/adhesive interface for the remaining paint systems.

Table 1. Physico-mechanical tests of the paint films

PVC/ vol. %	DFT/ µm	Impact/cm		Cupping/ mm	Adhesion/ °	Bending/ mm	Overall resistance/ %
		Front	Back				
DEPh/PANI							
1	90	100	100	10	1	4	100
3	90	90	100	10	1	4	99
5	90	90	100	10	1	4	99
10	115	70	100	10	1	4	97
15	120	65	100	10	1	4	94
17	120	55	100	10	1	4	93
Reference system: HCl/PANI PVC = 5 vol. %							

HCl/P.	90	50	100	10	1	4	92
Epoxy-ester resin							
nER	90	100	100	10	1	4	100

The results of measurement of Young's modulus of elasticity (E) indicate an appreciable effect of the epoxy-ester resin itself (E_{nER} = 2.27 GPa ± 0.1 GPa). From the increased value ($E_{DEPh/PANI\_1}$ = 4.2 GPa ± 0.2 GPa) it can be inferred that Young's modulus of elasticity was affected (increased) by the individual pigment particles and clusters in the paint, as also borne out by the 100 % resistance of the coatings in the mechanical tests. The modulus of elasticity $E_{HCl/PANI}$ = 0.7GPa ± 0.1 GPa is considerably lower than the E_{nER} value, which is consistent with the increased filling with the pigment particles, which cure the film but increase the film's brittleness. This conclusion is supported by the reduced resistance of the coating with HCl/PANI to the falling mass.

Local microhardness was determined by nanoscratch tests (Fig. 6). The material is inhomogeneous on the micro scale. Local microhardness of the various segments is different, depending on how much the site measured is affected by the pigment particles.

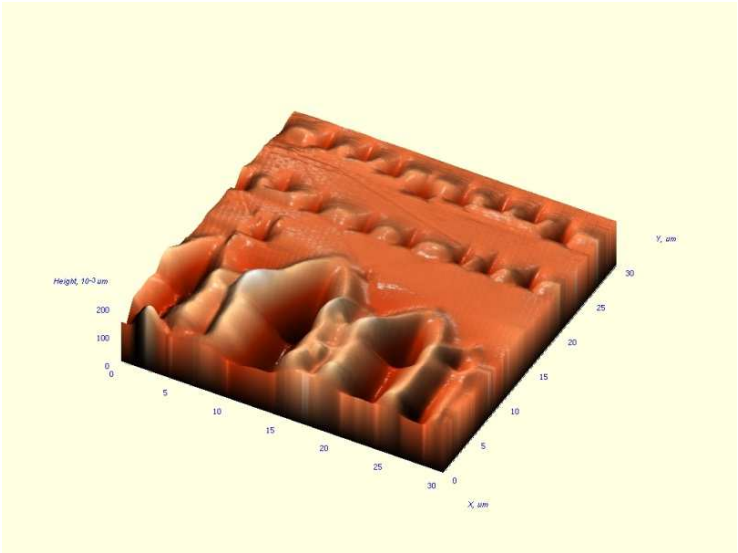

Fig. 6. DEPh/PANI_1 sample surface after nanoscratch tests (applied force 1 mN, 3 mN and 5 mN) and Young's modulus of elasticity (top). Scanned area 30 µm × 30 µm

Relative surface hardness (RSH) of the paint films is a next parameter measured as one of the mechanical tests. It was measured during 200 days, during which the majority of values attained a constant level (DEPh/PANI_1 and DEPh/PANI_15) while the remaining values exhibited a steadily increasing trend also after that time limit. All the values were converted to relative data with respect to the glass standard (RSH_{glass} = 100 %). The measurements were

made on 2 different measuring systems simultaneously and differences at the 10 % level were obtained, due to the design differences between the instruments. The second of the 2 systems, a König's apparatus, served to confirm the fact that the RSH of the paint films increases. The results are summarised in Table 2.

Table 2. Relative surface hardness of the paint films during 200 days

PVC/ vol.%	DFT/µm	Day of measurement									
		1	5	10	20	30	40	60	100	155	200
DEPh/PANI											
1	90	3.5	4	4.7	5.8	6.9	8.5	13.3	22.9	27.1	26.8
3	80	4.8	7.4	11.0	15.5	22.9	27.6	33.3	35.4	40.2	42.3
5	90	3.9	4.8	5.8	7.1	8.6	11.2	20.6	24.4	26.5	30.6
10	120	3.7	4.8	5.1	6.5	6.5	9.2	14.8	19	20.4	20.9
15	80	4.6	6.6	7.3	8.2	10.9	11.5	15.9	17.6	19.8	19.6
17	120	4.9	6.1	7.2	10.5	14.5	10.3	16.3	15.7	18.9	22.1
Reference system: HCl/PANI PVC = 5 vol. %											
HCl/P	80	5.9	7.9	9.1	16.9	27.3	34.7	33.7	40.8	42.7	43.1
Epoxy-ester resin											
nER	80	5.1	7.7	11.3	15.8	24.1	32.1	36.5	37.4	43.9	50.2

The nER film attained a 50 % level relative to the glass hardness in 200 days after application. Closest to this value was that of DEPh/PANI_3, viz. $RSH_{DEPh/PANI\_3}$ = 42.3 % (the values on the König's apparatus was 34.1 %; that of nER was 36.7 %). Any addition of the DEPh/PANI pigment makes the coating softer. The paint film hardness increases with increasing PVC up to PVC = 5 vol. % and starts to decrease slowly at PVC = 10 vol. %. The pigment particles exist in a tighter arrangement and the epoxy-ester resin binder does not fill the majority of the space any more (Fig. 7).

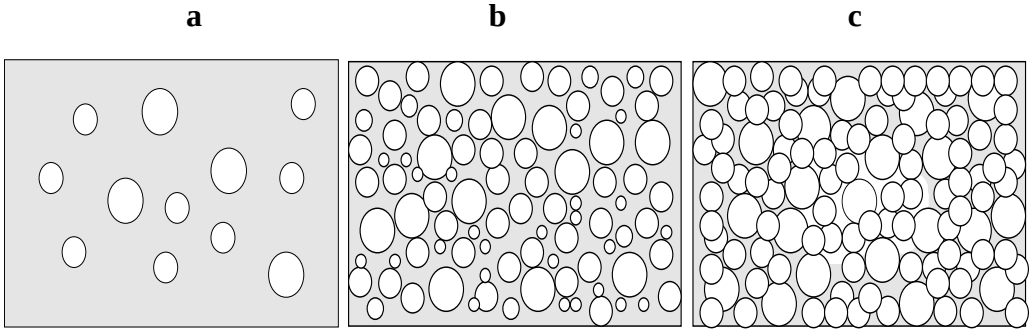

Fig. 7. Schematic arrangement of the pigment particles changing with increasing pigment concentration: (a) PVC < CPVC; (b) PVC ~ CPVC; (c) PVC ≥ CPVC

The ultimate goal of this work was to answer the question as to at which PVC the paint film provides the best corrosion protection to the steel substrate. It is generally believed that PANI type conductive polymers must not be present at too high concentrations to provide good anticorrosion protection (Kulhánková et al., 2014).

The parameters of aqueous extracts of the pigment powders and of the free paint films (including nER) were measured during 38 days, Table 3.

Table3. Pigment specification

Specification parameters	DEPh/PANI pigment
ρ/(g cm^{-3})	1.32
Oil abs per 100 g/g	101.65
CPVC/ vol. %	40.95
$M_{ws.c}$ / %	3.5
$M_{ws.h}$ / %	4.86
pH − day 0	4.32 ± 0.01 %
pH − day 21	2.65 ± 0.01 %
pH − day 38	4.82 ±0.01 %
χ − day 0/(µS cm^{-1})	489 ± 0.5 %
χ − day 21/(µS cm^{-1})	1160 ± 0.5 %
χ − day 38/(µS cm^{-1})	597 ± 0.5 %
x/(g L^{-1}); pH = 2.72	569.64
K_m/ %	96.21
U_R / %	1.27

The core of their preparation is in the preparation of the HCl/PANI pigment. The extract of the pigment alone was strongly acid (pH 1.46–1.59). (Note that diethyl phosphite is a substance of acid nature.) If combined with nER, the pH increased to pH ~4.32 during the 38 days; this pH approached closely that of the aqueous extract of the DEPh powder (pH 4.32−4.82). Both of the pigment extracts alone gave rise to high corrosion losses (HCl ~254 % and DEPh ~96 %), hence, introduction of DEPh to HCl/PANI brought about corrosion loss reduction (K_m = 96.21 %) and corrosion rate reduction (U_R = 1.27 %) nearly by one-third. If the paint with DEPh/PANI and with nER as the binder is formed, the U_R and K_m are more than 62 % reduced. The assumption of resistance of the nER film is also supported by the low corrosion loss data, which are due to the fact that the film contains no additives that may be released from the paint and support corrosion. The presence of substances soluble in cold water and in hot water increases the K_m and U_R values by 20 % in average ($M_{WS.c}$ = 3.5 %; $M_{WS,h}$ = 4.9 %). In a simultaneous measurement of acidity and alkalinity of the aqueous

extract of the DEPh/PANI pigment, the extract at pH 2.2 containing 569 g L^{-1} acidic components then had to be neutralised. They are residues of hydrochloric acid from the pigment preparation procedure, involving partial deprotonation of the PANI chain.

The aqueous extract pH, corresponding to the specific electric conductivity, is also important. It increases with increasing PVC. Conductivity increases with increasing PVC, i.e. with increasing concentration of initiators for cell formation (or a semiconductive material). The statement, that the higher conductivity, the higher anticorrosion protection is not always true. A conductive network must be formed, and this network will generate and consume just such a number of electron as is needed during the corrosion reactions. An optimum specific electric conductivity exists, and at the same time, the pH should approach as closely as possible the passivation level. The most resistant paint film, i.e. DEPh/PANI_10, exhibited (prior to steel panel insertion into the extract) pH 3.35 on day 21 and a more neutral value, pH 5.34, on day 38.

Point electron microanalysis (SEM, Bruker) was performed in order to verify the elemental composition of the top side of the DEPh/PANI_17 film. This analysis revealed the presence of phosphorus (2.79 mass %), oxygen (5.78 mass %), chlorine and sulphur (Fig. 8). They P and O values map the presence of phosphite in the film. Inorganic residues from the PANI pigment preparation process can be clearly seen. Chlorine 1.14 mass % hydrochloric acid residue and 1.02 mass % from the excess 0.5 M ammonium peroxodisulphate. Inorganics constitute roughly 10.7 mass % of the film matter, the remaining 90 % ± 1 % is the organic moiety. The last 2 elements could be detected as substances soluble in cold and hot water.

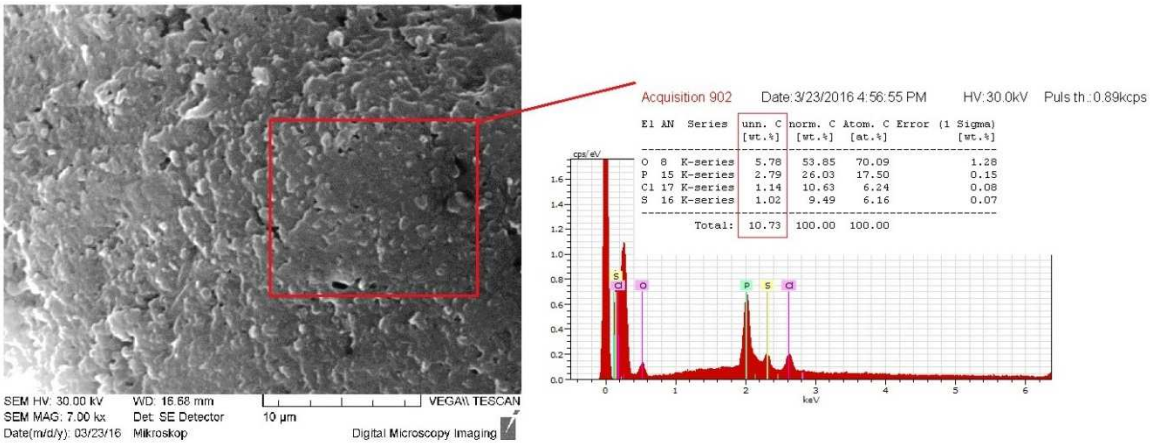

Fig. 8. SEM photograph of the analysed area of the DEPh/PANI_17 coating with electron microanalysis

All the paint films were subjected to the accelerated corrosion tests in the salt chamber (1344 h exposure), SO_2 chamber (1368 h exposure) and condensation chamber (3552 h exposure). The HCl/PANI and nER systems were also measured as reference materials.

Table 4. Results of the accelerated corrosion tests in the neutral salt spray environment (1344 h exposure)

PVC/%	DFT/µm	Blistering		Corrosion		Adhesion	Cut appearance	
		In a cut	Metal base	In a cut	Metal base	after expo.	before exposition	after exposition
		°	°			°		
DEPh/PANI								
1	170	6MD	6F	0.3	0.3	4	2	3a
3	180	6MD	4F	0.1	0.2	5	2	2
5	190	−	−	0.3	0.1	0	4a	1
10	200	−	−	1	0.4	0	4a	1
15	200	−	−	50	10	5	4b	2
17	210	−	−	10	0.1	0	4a	1
Reference system: HCl/PANI PVC = 5 vol. %								
HCl/P.	150	4F	2F	100	0.4	5	2	1
Epoxy-ester resin								
nER	150	4MD	2MD	1	0.7	4	2	3b

In the salt chamber, Table 4 the blister counts on the coating decrease with increasing PVC (from score 6MD to no blisters at all). This is also true of the blister count in the test cut area (count score F). Blisters were observed on the DEPh/PANI_1 and DEPh/PANI_3 pigmented films as well as on the nER film, where the blister density was higher (scored MD). Metal surface corrosion increases with increasing PVC up to PVC = 10 vol. % and exhibits a knee at PVC = 15 vol. %, where the corrosion is more extensive (50 %) than beneath the nER film (1 %). Corrosion in the cut is comparable, viz. up to 0.4 mm, only with the DEPh/PANI_15 film it is up to 10 mm, from which we deduce that PVC = 15 vol. % is a critical value for DEPh/PANI, the individual particles initiating penetration of the corrosive medium to the substrate metal. The 15% concentration was problematic only in the salt chamber, while the results observed at this concentration (and higher, PVC = 17 vol. %) in the two other chambers were good. Due to the large particle size (38 µm), a thicker paint film (200 µm ± 20 µm) had to be prepared for PVC = 15 vol. % and PVC = 17 vol. %. In an overall evaluation (comprising both the anticorrosion efficiency and mechanical efficiency), paints at the two PVC levels attain a score of 71 % and 82 %. Here the mechanism of protection against

corrosion is predominantly barrier type. The large dry film thickness (DFT) also contributes to a more difficult access of the corrosive medium to the substrate panel. The loss of paint film adhesion to the substrate at low pigment concentrations and at the above PVC as well as of the reference coatings poses the most important problem. The shape of the test cut was also assessed: panels with a better adhesion exhibited a poorer cut shape (score 4a−4b; Fig. 9), however, corrosion of the metal surface beneath the film was not very extensive and the cut shape exhibited score 1 on the visual assessment scale. The reason is in the formation of corrosion products of the Fe(II) and Fe(III) oxides, forming in the salt spray environment.
This trend does not hold in the corrosion environment with the SO_2 mist, Table 5.

Score	Corroded area
1 very small	
2 small	
3 a medium	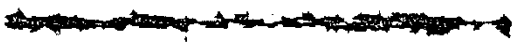
3 b	
4 a appreciable	
4 b	
5 very large	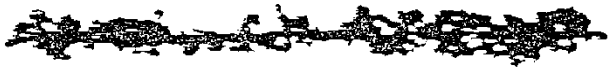

Fig. 9. Visual scale for cut appearance assessment

Table 5: Results of the accelerated corrosion test in the SO2 mist environment. Sample exposure time 1368 h

PVC/ vol.%	DFT/µm	Blistering		Corrosion		Adhesion	Cut appearance	
		In a cut	Metal base	In a cut	Metal base	after expo.	before exposition	after
		°	°			°		
DEPh/PANI								
1	170	2MD	2MD	10	0.5	4	2	4a
3	180	4MD	4M	3	0.6	5	2	4a
5	190	6F	−	3	0.3	5	2	3a

10	200	6F	−	16	0.3	0	1	4a
15	200	−	6F	3	0.3	0	2	2
17	210	4F	2F	10	0.3	0	1	4a
Reference system: HCl/PANI PVC = 5 vol. %								
HCl/P.	150	8F	4F	1	0.3	3	2	1
Epoxy-ester resin								
nER	150	2MD	2D	10	0.5	2	4a	3b

The results exhibit a proportional relation: poorer adhesion is accompanied by poorer test cut appearance, shifting from score 2 (before paint film removal) to score 3a−4a. In the SO_2 atmosphere, a larger blister size and a lower blister count (shift from 2MD to 4F) were observed at a higher PVC. This is a trend which is opposite to that in the salt chamber. The acid environment of the SO_2 chamber contributes to the substrate steel surface corrosion. Corrosion in the cut is nearly identical (0.3 %) for all the concentrations. The film adhesion loss effect occurs here like in the previous chamber. The paint films adhere better at higher PVC levels. The most resistant systems in the acid environment were DEPh/PANI_10 and DEPh/PANI_15 (anticorrosion efficiency 81 % and 87 %, respectively).

As to the samples continuously exposed in the condensation chamber (Table 6), increasing PVC is accompanied by decreasing blister counts and increasing blister sizes, both on the paint film surface (increasing trend from 4MD to 4F) and around the test cut (from 4M to 4F).

Table 6. Results of the accelerated corrosion test in the environment of condensed air humidity. Exposure time 3552 h

PVC/ vol. %	DFT/µm	Blistering		Corrosion		Adhesion	Cut appearance	
		In a cut	Metal base	In a cut	Metal base	after expo.	before exposition	after
		°	°			°		
DEPh/PANI								
1	170	4MD	4M	50	0.2	0	2	1
3	180	6M	4M	33	0.2	0	1	1
5	190	6M	6MD	10	0.2−0.3	0	2	1
10	200	8F	4F	3	0.2	0	1	2
15	200	8F	2F	3	0.3	2	1	2
17	210	6F	4F	3	0.2	2	2	1
Reference system: HCl/PANI PVC = 5 vol. %								
HCl/P.	150	6F	6MD	100	0−0.1	0	1	1
Epoxy-ester resin								

nER	150	6MD	6M	3	0−0.1	0	1	1

Substrate metal corrosion decreases with increasing PVC, amounting to 3 % at PVC = 10 vol. % − 17 vol. %. This may be due to the larger coat thickness and denser pigment particle distribution within the coat. Adhesion was outstanding in the case of the condensation chamber and the test cut appearance attained the unusually good score 2. Note that the sample exposure in the condensation chamber was 2.5 times than in the other chambers.

The DEPh/PANI_15 sample was analysed under a scanning electron microscope (Bruker) after 1561 h' exposure in the neutral salt spray environment. The analysis encompassed both the area around the test cut (Fig. 10) and an area beyond the test cut (Fig. 11).

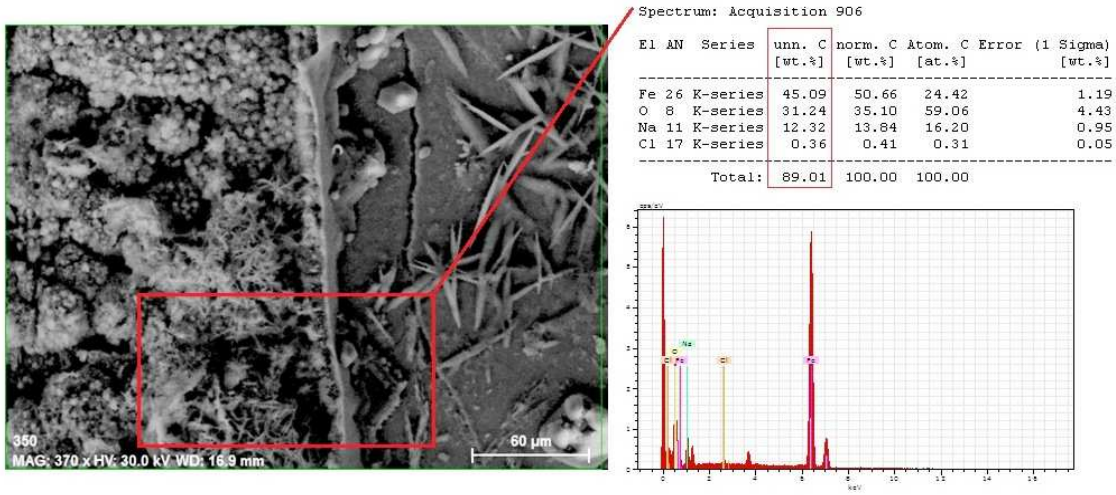

Fig. 10. SEM photograph with electron microanalysis of the DEPh/PANI_15 paint film in the area around the test cut

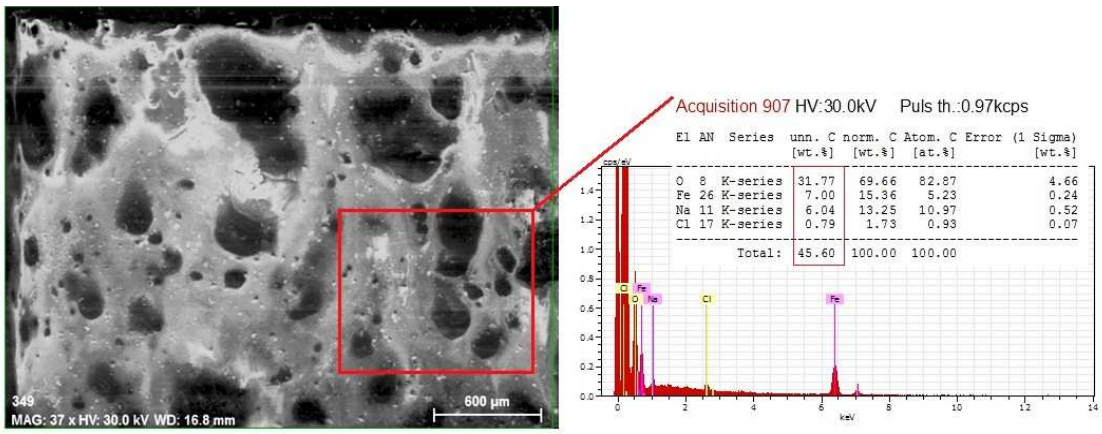

Fig. 11. SEM photograph with electron microanalysis of the DEPh/PANI_15 paint film on an area beyond the test cut

Elemental analysis of the coat surface was performed beyond the test cut area, and iron, oxygen, calcium and chlorine were detected.

X-ray analysis (Fig. 12) gave evidence of the presence of iron oxides, specifically Fe_2O_3 as maghemite and Fe_2O_4 as magnetite. According to the microanalysis, 38.77 mass % iron oxides were present beyond the test cut area and 76.33 mass % were present within the test cut area.

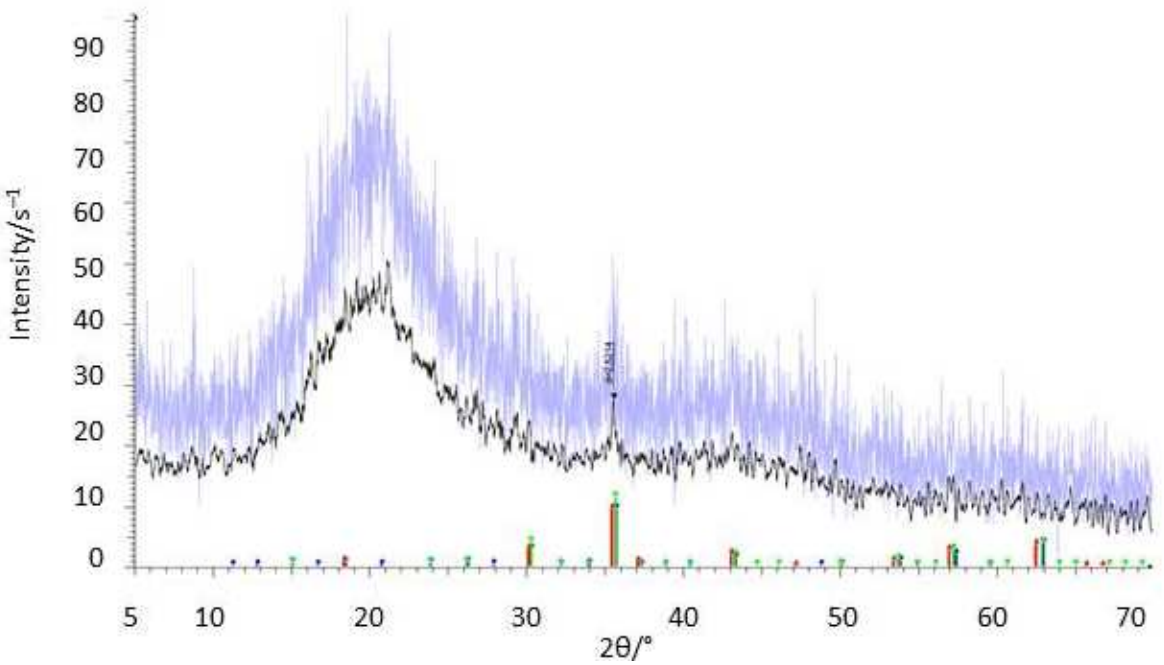

Fig. 12. X-ray analysis record of the back side of the DEPh/PANI_15 coating; exposition in NaCl chamber - 1561 h

The ferrous-ferric oxide layer was located on the bottom side of the paint film, i.e. on the substrate metal/film interface and played the role of a metal surface passivating layer preventing further penetration of the corrosive medium to the metal. Amorphous organic film was detected on the top of the coating. Precipitated salt residues from the salt chambers were also present on the coat surface, particularly in the test cut area, wherefrom they diffused into the near surroundings. The test cut surroundings contained 50 % more iron oxides, creating a passivating layer on the test cut.

Mechanical properties of the paint films were better at lower PVC values, where elasticity of the epoxy-ester resin binder played a more pronounced role. Lower pigment volume concentrations, however, are insufficient to prevent the corrosive medium from penetrating to

the substrate metal. Two corrosion protection mechanisms were found to act here: the barrier effect (pigment particles spread throughout the coat) and the electrochemical effect. The spontaneous corrosion potential E_{corr} increased with increasing PVC (E_{corr} = −304 mV and −309 mV for DEPh/PANI_5 and DEPh/PANI_10, respectively), polarisation resistance R_p was at the 1×10^5 Ω level. Those values are appreciably higher than the values of the commercially available TiO_2 paint at PVC = 50 %, which were E_{corr} = −573 mV and $R_p = 1 \times 10^1$ Ω. Corrosion rate is increased by electron exchange of the conductive polymer, where the paint film surface is sacrificed in favour of the substrate steel, as documented by the value for DEPh/PANI_10 where the corrosion rate increases from 10^{-3} mm year^{-1} to 10^{-2} mm year^{-1}.

Table 7. Calculated protective system efficiencies

PVC/ vol. %	NaCl/%	SO_2/%	H_2O/%	OAE/%	PMU/%	CAE/%
DEPh/PANI						
1	66	46	57	56	100	78
3	60	52	66	59	99	79
5	97	69	71	79	99	89
10	93	81	84	86	97	92
15	48	87	78	71	94	83
17	90	78	79	82	93	88
Reference system: HCl/PANI PVC = 5 vol. %						
HCl/P.	45	77	62	61	92	77
Epoxy-ester resin						
nER	51	51	73	58	100	79

Conclusions

This work was aimed at gaining a basic insight into the newly prepared DEPh/PANI system, with focus on the issue as to which pigment volume concentration in the epoxy-ester resin binder, provides the highest protective function, both from corrosion protection point of view and from the physico-mechanical strength point of view (Table 7). In the PVC = 1 vol. %, 3 vol. %, 5 vol. %, 10 vol. %, 15 vol. % and 17 vol. % series tested, the best results were observed at PVC = 10 vol. % (DEPh/PANI_10 system) and at PVC = 5 vol. % (DEPh/PANI_5 system). The combined anticorrosion efficiencies differed between those two systems by 3 %. While PVC = 5 vol. % is better from the physico-mechanical resistance aspect, PVC = 10 vol. % is more convenient from the anticorrosion protection aspect. The

optimum will thus lie between the two concentrations. The outstanding corrosion protection results obtained with the DEPh/PANI system are due to the fact that two mechanisms – the barrier mechanism and the electrochemical mechanism – are involved in this effect.

Symbols

B	benzoid structure	
CMX	Continous measurement of X	
D	dense (the highest frequency of the blistering of paint)	
DEPh/PANI	diethylphosphite with polyaniline base	
DEPh/PANI_1	coating of diethyphosphite with polyaniline base with PVC = 1 vol. %	
DEPh/PANI_10	coating of diethyphosphite with polyaniline base with PVC = 10 vol. %	
DEPh/PANI_15	coating of diethyphosphite with polyaniline base with PVC = 15 vol. %	
DEPh/PANI_17	coating of diethyphosphite with polyaniline base with PVC = 17 vol. %	
DEPh/PANI_3	coating of diethyphosphite with polyaniline base with PVC = 3 vol. %	
DEPh/PANI_5	coating of diethyphosphite with polyaniline base with PVC = 5 vol. %	
DFT	dry film tickness	
EB	emeraldime base	
$E_{DEPh/PANI\_1}$	Young's moduls of diethyphosphite with polyaniline base with PVC = 1 %	
EDX	Energy-dispersive X-ray spectroscopy	
$E_{HCl/PANI}$	Young's moduls of polyaniline hydrochloride	
E_{nER}	Young's moduls of nonpigmented epoxy-ester resin	
ES	emeraldine salt	
F	few (the lowest frequency of the blistering)	
HCl/PANI	paint of polyaniline hydrochloride	
K_m	corrosion loss reduction	%
M	medium (frequency of the blistering of paint)	
MD	medium dense (frequency of the blistering of paint)	
$M_{ws,c}$	presence of substances soluble in cold water	%
$M_{ws,h}$	presence of substances soluble in hot water	%
nER	nonpigmented epoxy-ester resin	
PANI	polyaniline	
Q	quinoid structure	
rpm	rotate per minut	
SEM	Scanning electron microscope	
UV	ultraviolet	
x	titration share of substances soluble in hot water	$g\ L^{-1}$

Greek Letters

ρ	density of pigments	$g\ cm^{-3}$

Subscripts

corr	corrosion
DEPh/PANI_1	coating of diethyphosphite with polyaniline base with PVC = 1 vol. %
DEPh/PANI_3	coating of diethyphosphite with polyaniline base with PVC = 3 vol. %
HCl/PANI	polyaniline hydrochloride
m	loss reduction
nER	nonpigmented epoxy-ester resin
R	rate
ws,c	soluble in cold water
ws,h	soluble in hot water

Reference

ASTM International. (2000) United States standard: Standard Test Method for Evaluation Degree of Blistering of Paints. ASTM D 714. West Conshohocken

ASTM International. (2008) United States standard: Standard test Method for Evaluating Painted or Coated Specimens Subjected to corrosive Environments. ASTM D 1654-92. West Conshohocken

ASTM International. (2012) United States standard: Practice for Evaluation Degree of Rusting on Painted Steel Surfaces. ASTM D 610-85. West Conshohocken

ASTM International. (2013) United States standard: Standard Practice for Conducting a Test of Protective Properties of Polish Applied to a Painted Panel Using Fluorescent UV-Condensation Light- and Water-Exposure Apparatus. ASTM D 1654-92. West Conshohocken

Ates, M., & Topkaya, E. (2015). Nanocomposite film formations of polyaniline via TiO_2. Ag. and Zn. and their corrosion protection properties. *Progress in Organic Coatings*, *82*, 33−40. DOI: 10.1016/j.porgcoat.2015.01.014.

Ayad, M.M., & Shenashin, M.A. (2003). Film thickness studies for the chemically synthesized conducting polyaniline. *European Polymer Journal*, *39*, 1319−1324. DOI: 10.1016/S0014-3057(03)00033-8.

Ayad, M.M., & Zaki, E.A. (2008). Dping of polyaniline films with organic sulfonic acids in aquaeous media and the effect of wather on these doped films. *European Polymer Journal*, *44*, 3741−3747. DOI: 10.1016/j.eurpolymj.2008.08.012.

Bedekar, A.G., Patil, S.F., Patil, R.C., & Vijayamohanan, K. (1997). Effect of monomer concentration and subsrate resistance on redox behaviour of polyaniline films. *Material Chemistry and Physics*, *48*, 76−81, DOI: 10,1016/S0254-0584(97)80082-X.

Cruz-Silva, R., Romero-Garcia, J., Angulo Sanchez. J.L.. Flores-Loyola. E., Farias, H.M., Castillon, F.F., & Diaz, A.J. (2004). Comparative study of polyaniline cast films prepared from enzymatically and chemically synthesized polyaniline. *Polymer,* 45, 4711−4717. DOI: 10.1016/j.polymer.2004.05.007.

Czech office for standards, metrology and testing. (1994) Czech technical standardMatallic and other non-organic coatings. Sulfur dioxide test with general condensation of moisture. CSN ISO 6988. Praha

Czech office for standards, metrology and testing. (1997) Czech technical standard: General methods of test for pigments and extenders - Part 10: Determination of density - Pycnometer method. CSN ISO 787-10. Praha

Czech office for standards, metrology and testing. (1997) Czech technical standard: General methods of test for pigments and extenders - Part 5: Determination of oil absorption value. CSN ISO 787-10. Praha

Czech office for standards, metrology and testing. (1997) Czech technical standard:. General methods of test for pigments and extenders - Part 9: Determination of pH value of aqueous suspension. CSN ISO 789-9. Praha

Czech office for standards, metrology and testing. (1997) Czech technical standard: Determination of oil absorption value. CSN 67 0531. Praha

Czech office for standards, metrology and testing. (2001) Czech technical standard:. General methods of test for pigments and extenders - Part 3: Determination of matter soluble in water - Hot extraction method. CSN ISO 789-3. Praha

Czech office for standards, metrology and testing. (2001) Czech technical standard:. General methods of test for pigments and extenders - Part 8: Determination of matter soluble in water - Cold extraction method. CSN ISO 789-8. Praha

Czech office for standards, metrology and testing. (2002) Czech technical standard: Paints and varnishes - Determination of resistence to humidity - Part 1: Continous condensation. CSN EN ISO 6270-1. Praha

Czech office for standards, metrology and testing. (2003) Czech technical standard:. General methods of test for pigments and extenders - Part 14: Determination of pH resistivity of aqueous extract. CSN ISO 789-14. Praha

Czech office for standards, metrology and testing. (2004) Czech technical standard: Paints and varnishes - Designation of quantity and size of defects, and intensity of uniform changes in appearance. CSN EN ISO 4628. Praha

Czech office for standards, metrology and testing. (2007) Czech technical standard: Paints and varnishes - Determination of film thickness. CSN EN ISO 2808. Praha

Czech office for standards, metrology and testing. (2007) Czech technical standard: Paints and varnishes - Cupping test. CSN EN ISO 1520. Praha

Czech office for standards, metrology and testing. (2007) Czech technical standard: Coating compositions. Determination of hardness of painting film by pendulum instrumen. CSN 67 3076. Praha

Czech office for standards, metrology and testing. (2012) Czech technical standard: Paints and varnishes - Rapid-deformation (impact resistence) tests. CSN EN ISO 6272. Praha

Czech office for standards, metrology and testing. (2012) Czech technical standard: Corrosion tests in artificial atmospheres - Salt spray tests. CSN EN ISO 9227. Praha

Czech office for standards, metrology and testing. (2013) Czech technical standard: Paints and varnishes - Cross-cut test. CSN EN ISO 2409. Praha

Czech office for standards, metrology and testing. (2014) Czech technical standard: Plastics - Methods of exposure to laboratory light sources. CSN EN ISO 4892. Praha

Dispenza, C., Sabatino, M.A., Deghiedy, N., Casaletto, M.P., Spadaro, G., Piazza, S., & Abd El-Rehim, H.A. (2015). In-situ polymerization of polyaniline in radiation functionalized polypropylene films. *Polymer, 67,* 128−138. DOI: 10.1016/j.polymer.2015.04.038.

Elkis, A.R., Gvozdenovic, M.M., Jugovic, B.Z., Stevanovic, J.S., Nikolic, N.D., & Grgur, B.N. (2011). Electrochemical synthesis and characterization of polyaniline thin film and polyaniline powder. *Progress in Organic Coatings*, *71*, 32−35. DOI: 10.1016/j.porgcoat.2010.12.004.

Gong, D., Dong, W., Hu, J., Zhang, X., & Jiang, L. (2009). Living polymerizatiom of 1.3-butadiene by a Ziegler-Natta type catalyst composed of iron(III) 2-ethylhexanoate. triisobualuminuum and diethyl phosphite. *Polymer*, *50*, 2826−2829. DOI: 10.1016/j.polymer.2009.04.038.

Grgur, B.N., Elkis. A.R., Gvozdenovic, M.M., Drmanic, S.Z., & Trisovic, T.L. (2015). Corrosion of mild steel with composite polyaniline coatings using different formulations. *Progress in Organic Coaing, 79*. 17−24. DOI: 10.1016/j.porgcoat.2014.10.013.

Huo, L.H., Cao, L.X., Wang, D.M., Cui, H.N., Zeng, G.F., & Xi, S.Q. (1999). Preparation and characterization of doped polyaniline. *Thin Solid Films,* 5−9. DOI:10.1016/S0040-6090(99)00293-X.

Jafarzadeh, S., Cleason, P.M., Sundell, P.-E., Tyrode, E., & Pan, J. (2016). Active corrosion protection by conductive composites of polyaniline a UV-cured polyester acrylate coatings. *Progress in Organic Coatings, 90*, 154−162. DOI: 10.1016/j.porgcoat.2015.10.008.

Kalendova, A., Vesely, D., Kohl, M., & Stejskal, J. (2014). Effect of surface treatment of pigment particles with polypyrrole and polyaniline phosphate on their corrosion inhibiting properties in organic coatings. *progress in Organic Coatings, 77*, 1465−1483. DOI: 10.1016/j.porgcoat.2014.04.012.

Kulhánková, L., Tokarsky, J., Matejka, V., Peikertova, P., Vallova, S., Mamulova Kutlakova, K., Styskala, V., & Capkova, P. (2014). Electrically conductive and optically transparent polyaniline/montmorillonite nanocomposite thin films. *Thin Solid Films, 562*, 319−325. DOI: 10.1016/j.tsf.2014.05.006.

Leymonie, J.P. (2007). Phosphites and phosphates: When distributors and growers alike could get confused. *Courtesy of New Ag International. Available from URL: http://www.spectrumanalytic.com/support/library/pdf/Phosphites_and_Phosphates_When_distributors_and_growers_alike_could_get_confused.pdf*

Liu, F.T., Neoh, K.G., Kang, E.T., Li, S., Han, H.S., & Tan, K.L. (1999). Effects of crosslink on polyaniline films doping behavior and degradation under weathering. *Polymer*, 40, 5285−5296. DOI: 10.1016/S0032-3861(98)00758-7.

Liu, X.H., Xia, Z.D., Zhou, H., Yuan, B., Li, Z., & Guo, F. (2013). Corrosion behavior of different steel substrates coupled with conductive polymer under different serving conditions. Journal of iron and steel research, International, 20, 87−92. DOI: 10.1016/S1006-706X(13)60147-8

Luo, J., Wang, X., Li, J., Zhao, X., & Wang, F. (2007). Conductive hybrid film from polyaniline and polyurethane-silica. *Polymer*, 48, 4368−4374. DOI: 10.1016/j.polymer.2007.05.062.

Motheo, A.J., Santos Jr,R.J., Venancio, E.C., & Mattoso, L.H.C. (1998). Influence of different types of acidic dopant on the electrodeposition and properties of polyaniline films. *Polymer*, 26, 6977−6982. DOI: 10.1016/S0032-3861(98)00086-X.

Mousavinejd, T., Bagherzadeh, M.R., Akbarinezhad, E., Ahmadi, M., & Guinel, M. J.-F. (2015). A novel water-based epoxy coating using self-doped polyaniline-clay synthesized under supercritical CO_2 condition for the protection of carbon steel against corrosion. *Progress in Organic Coatings, 79*, 90−97. DOI: 10.1016/j.porgcoat.2014.11.009.

Navarchian, A.H., Joulazadeh, M., & Karimi, F. (2014). Investigation of corrosion protection performance of epoxy coatings modified by polyaniline/clay nanocomposites on steel surfaces. *Progress in Organic Coatings*, *77*, 347−353. DOI: 10.1016/j.porgcoat.2013.10.008.

Olad, A. & Rashidzadeh, A. (2008). Preparation and anticorrosive properties of PANI/Na-MMT and PANI/O-MMT nanocomposites. *Progress in Organic Coatings*, 62, 293−298. DOI: 10.1016/j.porgcoat.2008.01.007.

Olad, A., & Nosrati, R. (2013). Preparation and corrosion resistance of nanostructured PVC/ZnO-polyaniline hybrid coating. *Progress in Organic Coatings*, 76, 113−118. DOI: 10.1016/j.porgcoat.2012.08.017.

Ozyilmaz, A.T., Akdaga, A., Karahan, I. H., & Ozyilmaz, G. (2013). The ingluence of polyaniline (PANI) coating on corrosion beheveiour of zinc-cobalt carbon steel electrode. *Progress in Organic Coatings*, *76*. 993−997. DOI: 10.1016/j.porgcoat.2012.10.020.

Ozyilmaz, A.T., Akdaga, A., Karahan, I.H., & Ozyilmaz, G. (2014). Electrochemical synthesis of polyaniline films on zinc-cobalt alloy deposited caron stell surface in sodium oxalate. *Progress in Organic Coatings*, *77*, 872−879. DOI: 10.1016/j.porgcoat.2014.01.020.

Sapurina, I., Mokeev, M., Lavrentev, V., Zgonnik, V., Trchova, M., Hlavata, D., & Stejskal, J. (2000). Polyaniline complex with fullerene C60. *European Polymer Journal*, *36*. 2321−2326. DOI: 10.1016/S0014-3057(00)00012-4.

Shauer, T., Joos, A., Dulog, L., & Eisenbach, C.D. (1998). Protection of iron against corrosion with polyaniline primers. *Progress in Organic Coatings*, *33*, 20−27. DOI: 10.1016/S0300-9440(97)00123-9.

Spinks, G.M., Dominis, A., & Wallace, G.G.(2003) Comparisoon of emeraldine salt, emeraldine base, and epoxy coatings for corrosion protection of steel during immersion in a saline solution. Corrosion, 59, 22−31. DOI: 10.5006/1.3277532

Stejskal, J.. & Gilbert, R.G. (2002). Polyaniline. Preparation of a conducting polymer. *International union of pure and applied chemistry*, *74*, 857−867. DOI: 10.1351/pac200274050857.

Špírková, M., Brus, J., Božanová, L., Strachata, A., Baldrian, J., Urbanová, M., Kotek, J., Strachová, B., & Šlouf, M. (2008), A view from inside onto the surface of self-assembled nanocomposite coatings. *Progress in Organic Coatings*, *61*, 145−155. DOI: 10.1016/j.porgcoat.2007.07.032.

Tokarsky, J., Maixner, M., Peikertova, P., Kunhankova, L., & Burda, J.V. (2014). The IR and Raman spectra of polyaniline absorbed on the glass surface; comparison of experimental.

empiral force field and quantum chemical results. E*uropean Polymer Journal*, *57*, 47−57. DOI: 10.1016/j.eurpolymj.2014.04.023.

Yang, X., Li, B., Wang, H., & Hou, B. (2010). Anticorrosion performance of polyaniline nanostructures on mild steel. *Progress in Organic Coatings*, *69*, 267−271. DOI: 10.1016/j.porgcoat.2010.06.004.